Heat Rejection Capacity in Miniature Thermoacoustic Expanders at Cryogenic Temperature 77 K

Zhimin Hu
CryoWave Advanced Technology, Inc.
Woonsocket, RI 02895

T. Roberts
Air Force Research Laboratory AFRL/RVSS
Kirtland AFB, NM 87117

ABSTRACT

Miniaturized thermoacoustic expanders MTAEs are a new type of expander designed to improve the cooling efficiency of recuperative type cryocoolers without sacrificing their reliability and simplicity. Experimental studies have demonstrated the feasibility of MTAEs, including their ability to remove heat from the expansion of a DC cold-stage flow to a high-temperature reservoir. The heat pumping from the cold-stage to a hot sink by an MTAE relies critically on the behavior of nonlinear wave systems created in miniature-scale channels (several hundreds microns) inside resonant tube bundles of MTAEs. This paper presents an experimental investigation of this heat rejection capacity between a low temperature source and a much higher temperature sink and the influence of such heat energy pumping on the cooling performance of an MTAE operated at a cryogenic temperature of 77 K. The objective is to explore this technology's feasibility in both scaled down and cryogenic temperature conditions. The characteristics of acoustic wave systems and the cooling power achieved using helium in the MTAE (170 mg/s) with different supply pressures and hot reservoir temperatures are reported. The observations and challenges of the thermoacoustic streaming phenomenon and modeling in miniature or micron-scale channels is also discussed.

INTRODUCTION

Cryocoolers are a key component of space-based IR sensing systems. A long-life, reliable, and efficient cryocooler system is an enabling technology for providing cryogenic cooling of detectors and optics that are integral to space surveillance missions involving IR payloads. The operational requirements stemming from such missions serve a critical function of stimulating many of the cryocooler technology development efforts such as this one. Key cooler development issues include vibration free operation, reliability, efficiency of operation, and flexibility of the thermal management system to deliver cooling power to remotely located loads or to multiple payloads for long-term missions.[1-9]

In the past two decades, the developments of cryocooler systems have dramatically improved cryocooler reliability and efficiency by eliminating mechanical moving parts at cold stages in re-

Cryocoolers 16, edited by S.D. Miller and R.G. Ross, Jr.

generative-type cryocoolers (pulse tubes); this resulted in revolutionizing infrared space missions. The increasingly dominant pulse tube cooler has largely supplanted other thermodynamic cycles in space applications due to elimination of moving parts from the cold stages. Reverse turbo-Brayton and Joule-Thomson coolers, which are the typical recuperative cryocoolers employed in IR systems, have successfully demonstrated their feasibility in space missions.[8-10] In spite of challenges to miniaturizing mechanical expanders due to parasitic inefficiencies and mechanism complexity, the reverse turbo-Brayton cooler still is a very competitive solution due to its high cooling efficiency for large cooling loads at low temperatures below 10 K. One of the advantages of recuperative cryocooler systems is the separation of the compression unit from the expansion device at the cold-stage, as allowed by the DC flow inherent in such systems. This separation is also useful in reducing the vibration at the cold stage that is intrinsically created by the compression unit, thus improving the performance and accuracy of the IR system.

Improved efficiency of recuperative coolers is also a significant direct benefit for IR systems by reducing the payload and power consumption. In a recuperative type of cryocooler system, cooling power critically depends on the efficiency of the expander at the cold stage.[5-10] The more energy (either work or heat) that is removed by the expander at the cold stage and transported to high-temperature reservoirs (hot sink), the more cooling power is produced without adding input power to the system. Thus, assuming the system recuperators (DC flow heat exchanges) are very efficient, we have concluded that improving the extraction of work directly from the cold stage expansion is the only effective way to improve the efficiency of recuperative cryocoolers.

Traditionally, high efficiency expansion devices are usually accomplished by using mechanical mechanisms (rotary or reciprocating moving parts) that are designed to convert the pressure energy into mechanical work, thus minimizing thermodynamic-irreversibility in the expansion process. However, it is clear that the use of mechanical moving parts in the cold stage not only increases system complexity and cost, but also reduces the reliability of the cryocooler. The problem of mechanical expanders is further intensified as attempts are made to miniaturize them for smaller IR applications. In fact, to retain or improve the cooling efficiency of low cooling capacity recuperative coolers using existing technologies is a serious challenge because:

- The efficiency of mechanical expanders intrinsically decreases when they are scaled down to miniature dimensions (micrometers) due to relative increases in parasitic flow losses and thermodynamic-irreversibility.
- The difficulty of fabricating mechanical structures of expansion devices when scaled down to miniature dimensions (micrometers).

As a result, the isenthalpic type of expander, such as the Joule–Thomson expander, including capillary tubes, orifice passage, and porous plugs, is often the only feasible choice for miniaturized recuperative cryocooler systems (<1W). This is because of its ease of scaling, simple structure, and no moving mechanical parts. As a matter of fact, any type of isenthalpic expander is essentially a flowing resistant component that functions to dissipate the kinetic energy of the coolant created from expansions. Except for the advantages aforesaid, this type of expander offers maximum inefficiency of cooling generation for miniaturized recuperative coolers due to its intrinsic thermodynamic irreversibility.

Addressing these recuperative expander challenges by reducing thermodynamic irreversibility in miniaturized expansion devices for recuperative coolers is the motivation for the current research. A miniaturized thermoacoustic expansion technology has been developed that features a simple structure with no moving parts, is scalable to smaller applications like J-T expanders, and has the capability to remove work from the expansion process so as to improve and cooling efficiency like mechanical expanders. The technology combines the advantages of both isentropic and isenthalpic expansion devices and provides a new solution for miniature recuperative coolers for future use in space-borne telescopes and infrared instruments.

Cryowave Advanced Technology has been developing this miniaturized thermoacoustic expansion technology since receiving funding from a DoD SBIR program in 2007. This paper reports the recent progress made on the experimental study of MTAE feasibility and operability at a cryogenic temperature of 77K. The prototype experiments demonstrate that the MTAE thermoacoustically

extracted work from a dc gas flow can create approximately 2W of cooling power at the cold stage temperature of 77 K, while rejecting the heat to a heat sink with a temperature between 200 K to 280 K. The experiments also verified that the MTAE produces cooling power at 77 K, outside of the inverse temperature envelope of a conventional J-T expander run with helium gas without precooling. The successful development of MTAEs potentially brings direct benefits for space missions because the technology is applicable over a wide temperature range, allowing its use for SWIR, MWIR, and LWIR surveillance and interceptor systems.

MTAE MECHANISM & HEAT PUMPING

In a recuperative cryocooler, the efficiency of the expander at the cold stage crucially determines the cold-stage temperature and output cooling power. The MTAEs objective is to improve cooling efficiency by using a new approach that achieves a quasi-isentropic reversible expansion. MTAEs use acoustic wave systems that replace the moving parts used in conventional isentropic expanders to transport work from the expansion at the cold stage. The operational mechanism in a MTAE was introduced previously[11,12] and is briefly described below.

An MTAE consists mainly of three parts: nozzle, oscillation chamber, and resonant tube-bundle. As a dc-flow supply gas enters an MTAE device, an isentropic reversible expansion is carried out in the nozzle that produces a temperature drop in the gas. In the oscillation chamber, an intensive acoustic wave system is driven by the interaction of the low-temperature, high-speed jet coming out from the nozzle with a resonant-tube bundle downstream. The dc-flow supply gas is then turned into ac-flow in the resonant tubes to form the intensive acoustic wave system. The formed acoustic wave system in each of the resonant tubes turns the acoustic streaming into heat at its hot end that is pumped out of the device through its heatsink conduction interface. By means of acoustic wave systems, the pressure energy that is usually dissipated locally in conventional J-T expanders is now used to remove the heat of expansion in the MTAEs. For a better understanding of the heat pumping processes, a schematic illustrating the MTAE mass streaming and energy transport is given in Fig. 1.

The mass streaming through an MTAE is given by the U-shaped dotted line in Fig. 1; this represents the dc supply-gas flowing in and out of the device. The energy streaming (enthalpy) along with the mass streaming (m_{in}) in the MTAE device is indicated by the adjacent lower solid U-shaped arrow. The work (enthalpy streaming) removed from MTAEs is depicted by the dotted line pointing to Q_H. As seen in Fig. 1, the mass streaming remains conservative as it flows in and out of the device by a short passage (nozzle and oscillation chamber). In contrast, the total enthalpy streaming ($H_{in} = m \cdot h_{in}$) carried with the mass streaming given by H_{in} for inflow and H_{out} for outflow is not conservative because a portion of the enthalpy is removed by acoustic streaming to the hot end of the device as indicated by the dotted line pointing to Q_H.

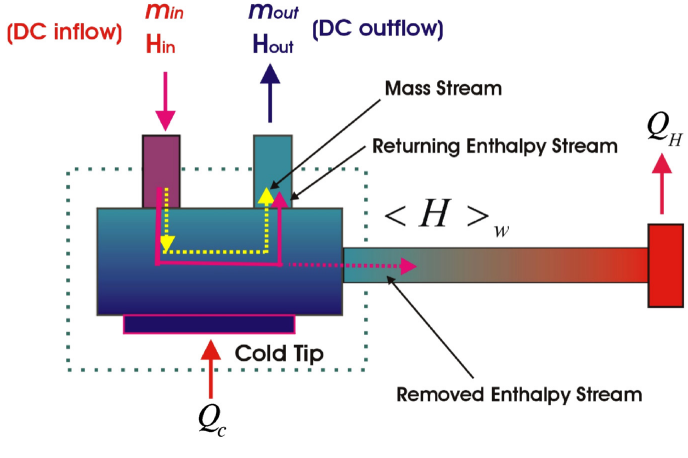

Figure 1. Schematics of MTAE Operations.

The enthalpy difference through the MTAE device is given by ΔH

$$\Delta H = H_{in} - H_{out} \tag{1}$$

The total enthalpy change (ΔH) through MTAE expansion in real gases is attributed to two contributions:

$$\Delta H = < \Delta H >_w + < \Delta H >_r \tag{2}$$

The enthalpy steaming $<\Delta H>_w$ is energy exchanging through the device boundary (*extracted from the cold stage by expansion engines*), and the intrinsic enthalpy change $<\Delta H>_r$ is related to thermodynamic states in real gases. Here $<\Delta H>_w = Q_h$ is for MTAE, and $<\Delta H>_w = W$ is for a mechanical expander. The intrinsic enthalpy change due to expansions is given by

$$< \Delta H >_r = [H_{out}(T_{out}, P_L) - H_i(T_{in}, P_H)] \tag{3}$$

Thus the cooling power Q_c at the cold-stage temperature T_c is generally estimated by

$$Q_c = < \Delta H >_w + < \Delta H >_r \tag{4}$$

For a cryocooler using J-T expanders, a finite refrigeration power only occurs with a real gas due to no expansion work and heat extracted

$$< \Delta H >_w = 0 \tag{5}$$

To assess the capacity of MTAE heat pumping in a cryocooler, the maximum work ($W_{c,max}$) that is available to be removed from expansion usually is estimated. The maximum work equals the work input required to reverse the isentropic expansion from the cold-stage to the supply pressure

$$W_{c,\max} = \dot{m} \frac{\gamma}{\gamma - 1} R T_c [(P_H / P_L)^{\frac{\gamma - 1}{\gamma}} - 1] \tag{6}$$

where R is the specific gas constant, and γ is the specific heat ratio of working gases. The actual power of MTAEs extracted in terms of acoustic streaming will be some fraction of the maximum work $W_{c,max}$ due to inefficiencies of the expansion processes. The MTAE expansion efficiency is given by

$$\varepsilon_T = \frac{< \Delta H >_w}{W_{c,\max}} \tag{7}$$

Provided that the specific heat variation of the supply gases through the pressure drop are ignored, the expansion efficiency can be then estimated directly by the measurement of temperature change between the inlet and outlet of the device. The MTAE efficiency is thus calculated by

$$\varepsilon_T = \frac{T_{in} - T_{out}}{T_{in} - T_s} \tag{8}$$

where T_{in} and T_{out} are the temperature in both inlet and outlet streams respectively. T_s is the outlet temperature incurred in reversible isentropic expansion under the same operating conditions. Obviously the more heat that is removed by MTAEs, the lower the temperature that is obtained, and the more cooling power that is produced in the cold stage of the recuperative cooler system. To detail the heat pumping by the acoustic wave system in an MTAE, a parameter describing the energy dissipation rate related to one acoustic pulse is introduced. It is defined by

$$< \Delta H >_f = \frac{< \Delta H >_w}{f_n} \tag{9}$$

where f_n is the highest-frequency component present in the resonant tubing bundle. The $< H >_f$ represents the fraction of enthalpy streaming pulled out from steady dc flow by each acoustic pulse during heat pumping. Because the nonlinearity of intensive acoustic wave systems is accompanied with heat pumping and dissipation, acoustic energy is shifted from the low frequency band to higher orders of wave components as the acoustic waves propagate.

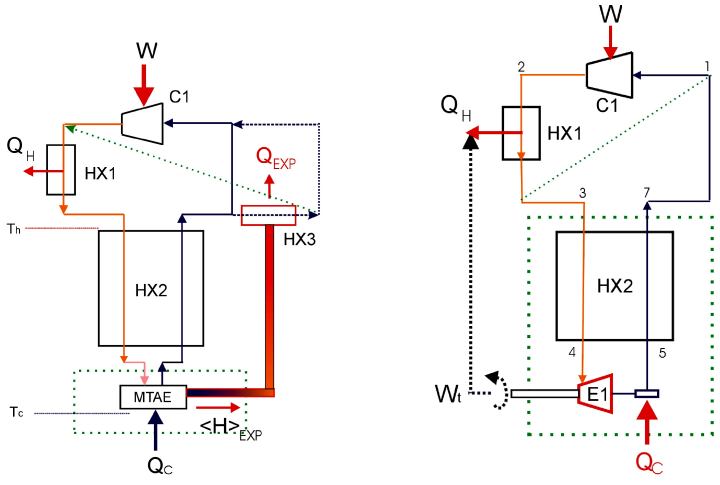

Figure 2. Thermoacoustic expansion cooling system using MTAE *(left)* vs. reverse turbo-Brayton cycle using mechanical expander *(right)*.

A recuperative cryocooler system in which an MTAE substitutes for a J-T expander is illustrated in Fig. 2 (left) as compared to a reverse turbo-Brayton cycle in Fig. 2 (right). The requirements on the temperature level and heat pumping capacity of this system are defined so as to make the MTAE cooler competitive for a small scale system. For this system, the MTAEs are required to reject the heat removed from expansion to the temperature level of the returning gas out of the recuperator on the compressor side. The maximum system efficiency and minimum power input of this cryocooler will be reached if the MTAE is able to reject its heat at the temperature of the heat exchanger HX1 of the compression unit.

The cooling power output from three recuperative cryocoolers systems that use three different expanders (J-T expander, turbo-expander, and MTEA) are given in Eqs. (10) to (12):

$$Q_{c\_JT} = < \Delta H >_r \tag{10}$$

$$Q_{c\_EXP} = W_t + < \Delta H >_r \tag{11}$$

where $< \Delta H >_w = W_t$ as given in Eq. (4)

$$Q_{c\_MTAE} = Q_{\exp} + < \Delta H >_r \tag{12}$$

where $< \Delta H >_w = Q_{\exp}$ as replaced in Eq. (4). Apparently, the cooling power of an MTAE cryocooler increases in proportion to the removal of heat by the cold-stage expander. Provided that J-T expanders have zero-adiabatic-efficiency and mechanical expanders have higher isentropic efficiency than MTAEs in favorable operating conditions of mechanical expanders, the cooling power output is easily assessed by Eq. (13):

$$Q_{c\_JT} < Q_{c\_MTAE} \le Q_{c\_EXP} \tag{13}$$

For the MTAE cryocooler system given in Fig. 2, Eq.(12) suggests that the MTAE heat rejection under cryogenic conditions plays a crucial role in enhancing the cooling power for miniature cryocooler systems. In essence, the temperature at which heat is rejected will determine the feasible operational conditions for the system.

Next, we describe results of experiments that were designed to examine the capacity of MTAE heat rejection under different heat rejection temperatures so as to evaluate the cooling performance in response to the temperature of the heat sink.

EXPERIMENTAL SETUP

To verify the heat pumping capacity of the MTAEs under 77 K conditions, a testing system was fabricated, as shown in Fig. 3. The system was designed to work with the MTAE prototype in

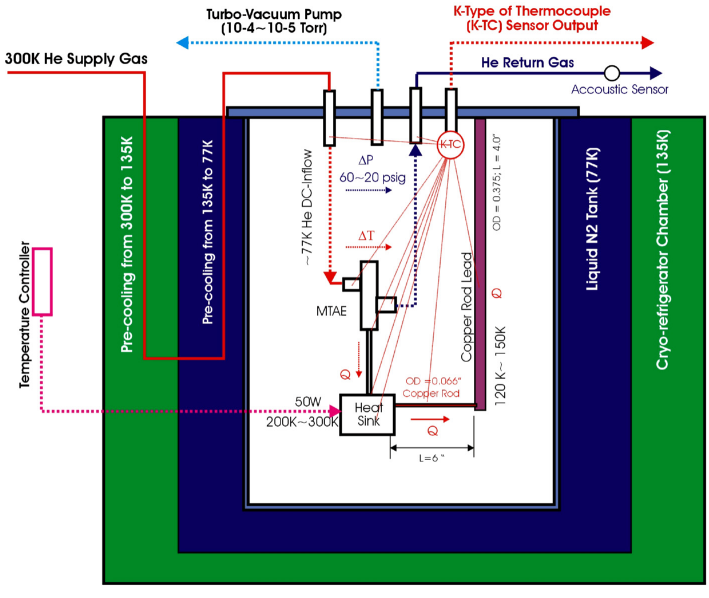

Figure 3. Illustration of setup of MTAE Heat Pumping Tests.

experiments covering the full temperature range from 300 K to 77 K. The testing setup mainly consists of a 135 K cryo-refirgerator-cooled chamber, an LN_2 tank and adjoining 77 K vacuum chamber, and a refilling system that provides a precooling supply gas stream for 77 K tests. The small 77 K vacuum chamber provides the vacuum environment for thermal isolation of the tested prototype and is installed inside the LN_2 tank. The MTAE prototype was installed inside the 77 K vacuum chamber with several temperature sensors (K-type of thermocouple with OD=0.003" and 0.010" respectively). A Lakeshore 331 temperature controller and a 50 W electric heater were mounted to the heat radiator of the MTAE prototype through a feedthrough extended out from the 77K vacuum chamber and 135K chamber by a six-foot copper tubing.

The LN_2 tank and 77 K vacuum chamber in the testing system is pictured in Fig. 4. The heat radiator (heat sink) of the MTAE is connected by a copper wire (OD=1/16") that was anchored to the 77 K vacuum chamber flange through a copper rod (OD=3/8"). The copper wire combined with the electrical heater (50W) formed the stable heat shunt to maintain and adjust the temperature on

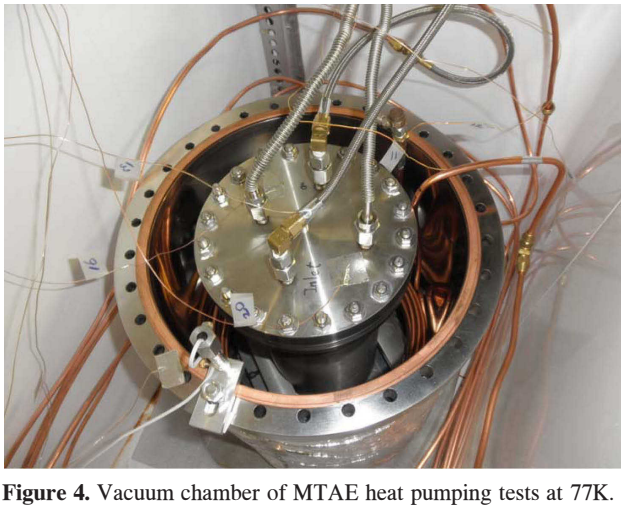

Figure 4. Vacuum chamber of MTAE heat pumping tests at 77K.

the heat radiator, thus simulating the MTAE device's operation between the temperature span given by the supply gas stream (at cold-end of a recuperator) and the hot reservoir (heat reject temperature). The heat streaming out of the 77 K vacuum chamber is controlled by the heat conduction rate over the length of the copper wire. It is observed that before the MTAE begins operation, there is a steady heat flux provided by the electrical heater that flows in both the MTAE body and the copper wire.

The following testing steps were taken during the MTAE heat rejection experiments:

- Running 135 K cryo-refrigerator to precool down the supply gas (He) and shield the whole LN_2 tank and 77 K vacuum chamber inside the cryogenic-refrigerator chamber at 135 K;
- After the system is stabilized, tuning the MTAE prototype with 135 K supply helium gas;
- After the oscillating mode and cooling performance are verified at 135 K, filling LN_2 tank to further cool down the supply gas to 77 K;
- After the system is stabilized, running supply gas (helium) with very low pressure (<5.0 psig) and flow rate that will not drive the oscillating mode so as to calibrate the temperature sensor inside the MTAE body (*The reading will reflect the temperature effect of helium gas before its inversion temperature is reached*);
- Set the supply gas to the testing pressure;
- After the 77 K vacuum chamber and MTAE prototype were stabilized under the supply pressure, the temperature and pressure were measured and acquired by an HP 34970A data acquisition system;

EXPERIMENTAL RESULTS

Several MTAE prototypes were fabricated and tuned-up between 300 K and 135 K so as to verify the geometries of the oscillation chamber and resonant tubes before the 77 K experiments were performed. A successful configuration of oscillating chamber and resonant tubes results in a stable oscillating mode and efficient cooling performance as the device cools down with the supply gas temperature to the cryogenic testing temperature. Thus, the device is at first tuned at ambient temperature to properly match the micro-jet with the resonant tube in order to drive the oscillating mode. After the oscillating mode is triggered, the procedure of heat pumping is examined together with the temperature drop between the inflow and outflow streams. Using helium supply gas, the oscillating mode and cooling effects are more easily detected because helium has a much higher sound speed than other gas types at ambient temperature. The configuration of the oscillation chamber depends on the type of supply gas and its sound speed.

It is worth noting that as the device is scaled down in size, detecting the micro-jet structure in the expansion state throughout the temperature span becomes very challenging due to the scale of the nozzle. Empirically, it has been demonstrated that the operational mode with the needed jet oscillation critically relies on the acoustic characteristics of the resonant tube bundle that form the feedback loop to drive the spontaneous oscillations of the jet structure and gas column. As a result, the MTAE is first experimentally tuned between 300 K and 135 K by adjusting its interior structure and nozzle size. After successfully tuning up the MTAE prototype at 135 K, the device is continuously cooled down to 77 K using liquid nitrogen, and the cooling performance and heat removal is examined. The preliminary testing results of MTAE heat rejection at 77 K are presented in this section.

In Fig. 5, the variation of cooling power versus the temperatures of the heat rejection radiator is presented. The cooling power output is estimated by the temperature drop measured in the gas streams (not on the exterior conduit body) in both inflow and outflow of the device. The upper solid line marked 60 psig indicates the cooling output of the prototype when driven by 60 psig helium at the inflow temperature of 78 K. The lower solid line marked 50 psig gives the MTAE cooling power driven by 50 psig helium at the same temperature. It is apparent that the MTAE cooling power declines when the temperature of the heat sink goes up. Notice that, at a heatsink temperature of 280 K, the cooling power vanished with 60 psig helium if the measuring error of the thermocouple is included, which is plotted by the horizontal dotted line. Interestingly, when the heatsink

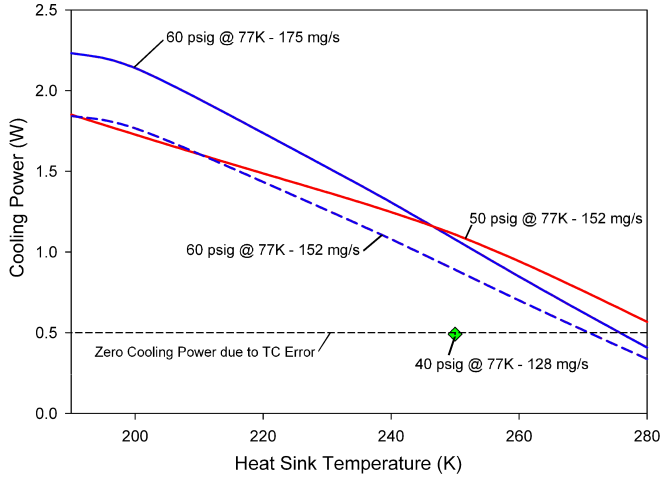

Figure 5. MTAE cooling power output vs. heat pumping temperature at 77K (*supply gas: He).*

temperature is above 250 K, if the supply helium pressure is lowered from 60 psig to 50 psig, the MTAE cooling power increases instead of decreasing. The cooling power degradation might be the result of a mismatch of resonant conditions between the micro-jet and the resonant tube caused by a local change of sound speed over the temperature distribution of the gas column. It indicates that there exists an optimal operating condition when cooling power is maximized in matching the 10 micro-jets with the resonant tubing geometry as the device cools down from high to low supply gas temperature. Also, the reduction of supply gas pressure results in lowering the mass flow rate through the MTAEs.

The lower dashed line in Fig. 5 indicates the cooling power for 60 psig supply gas when scaled for the same mass flow rate that was measured for the 50 psig supply gas case. Compared with the cooling power at 50 psig (solid-line with the same mass flow rate), it is clear that less cooling power per unit mass flow is obtained for the 60 psig case.

The temperature drop and cooling power for various cold stage inflow pressures at 77 K are plotted in Fig. 6 for a 250 K heat sink temperature. Note that this plot also shows the phenomenon of highest cooling power being achieved for pressures around 50 psig. The two lines in Fig. 6 present the output of the MTAE cooling power and the temperature drop created by the device as

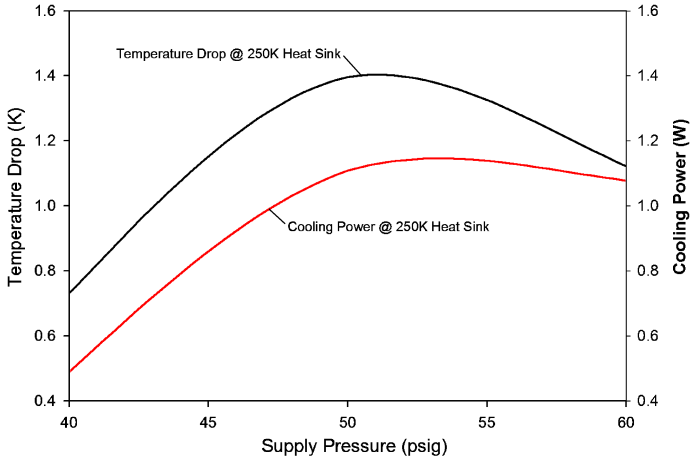

Figure 6. Temperatures drop and cooling power at 77 K vs. heat pumping to 250 K heatsink (*Supply gas: Helium*)

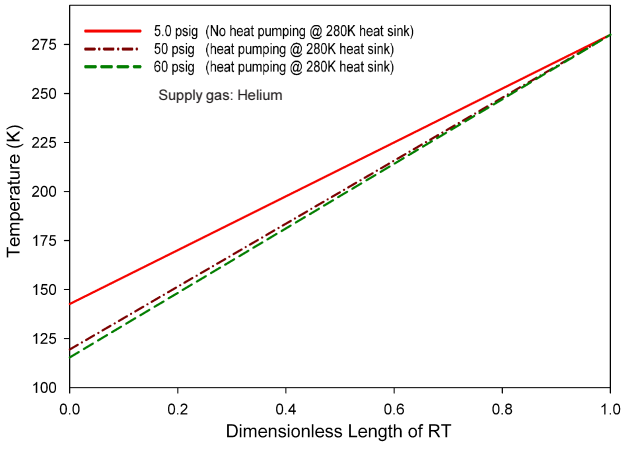

Figure 7. Temperature on RT surface from 77 K cold-stage to 280 K heatsink.

the helium supply pressure changes between 40 psig and 60 psig. As seen, the largest temperature drop is produced at around 50 psig. This means that, as the supply pressure increases and available work increases, the expander does not perform effectively to produce more cooling power from the increased work. The additional work is turned to heat added to the outflow stream instead of increase cooling power; i.e. thermodynamic irreversibility increases and temperature increases due to expansion occurring in the temperature region where the J-T coefficient for helium is negative.

The heat pumping capability of the MTAE was also evaluated by noting the variation of temperature along the resonant tubes bridging between the 77 K cold stage and the 280 K temperature of the heat sink. The temperature distribution varies with pressure drop as shown in Fig. 7. The top solid-line indicates the temperature distribution on the RT surface under conditions of zero cooling power output in which a small volume of low-pressure (5 psig) helium is fed through the device. With this supply pressure, there is a weak isenthalpic expansion that occurs in the MTAE which does not create any temperature change between the inflow and outflow. It provides a stable thermal balance condition along the RT surface due to zero heat flux transported from the cold end to hot end of the resonant tube.

The middle dot-dashed line in Fig 7 represents the temperature distribution along the RT surface when driven by an inflow of 50 psig helium at 77 K. The temperature at the cold end of the RT surface drops 23 degrees compared to the temperature on the cold end of RT surface with zero-heat flux. The temperature at the hot end of RT surface remains constant as it is anchored to the 280 K heat sink.

The bottom dashed line in Fig. 7 is the temperature distribution along the RT for 60 psig supply gas. Note that it created a lower temperature for the cold end of the RT surface than did the 50 psig case. As seen, as the supply pressure increased, the temperature on the cold end of the RT surface decreased due to heat being transported to the hot end of the RT surface as driven by the interior acoustic system.

At this point we introduce the parameter α that gives the ratio of the temperature drop over the extended RT length to the temperature drop between the cold stage and the MTAE heatsink. This ratio is defined by

$$\alpha = \frac{DT_{RT}}{DT_{MTAE}} \tag{14}$$

where DT_{RT} is the temperature drop across the extended RT length, and DT_{MTAE} is the temperature difference between the cold stage and the heatsink where the MTAE pumps its heat. The variation of this ratio versus the heat sink temperature is examined in the experiments and the results are plotted in Fig. 8.

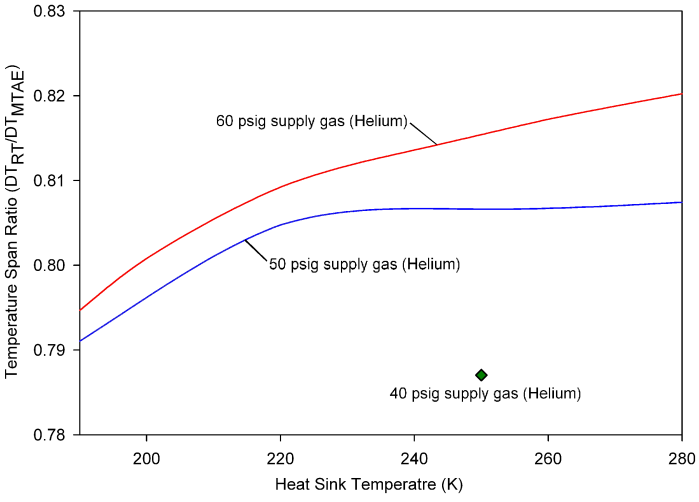

Figure 8. Ratio of temperatures span over RT at 77 K vs. heatsink temperatures.

The temperature span ratio (α), as shown in Fig. 8, indicates the capability of the extended RT structure to transport heat and pump it to the heatsink. The two curves in the plot give the variation of this ratio with heatsink temperature for two supply gas pressures: 60 psig and 50 psig. It is seen that the larger the value of the parameter, the smaller the temperature rise in the MTAE body, which indicates that the extended RT length out from the body dissipates more acoustic streaming than the part of the RT in the MTAE body. It is also observed that, as supply pressure drops, the heat pumping and acoustic dissipation on the extended RT section is significantly degraded at the 250K heat sink. Also the heat dissipation and rejection at the hot end of the extended RT becomes weak as the temperature of the heatsink increases from 240 K to 280 K for the 50 psig supply pressure.

CONCLUSIONS

Preliminary experimental studies on the capacity of MTAE heat pumping have been performed at a cryogenic temperature of 77 K. The tested prototype was designed and fabricated to handle a flow rate in the range of 140 mg/s to 175 mg/s at 77 K. The experiments demonstrated that the MTAE prototype, when driven by helium supply gas, provided a cooling power of 0.8 W at a flow rate of 152mg/s, and was able to pump this heat from the 77 K cold stage to the 250 K heatsink. The prototyped MTAE was also able to deliver a cooling power of 2 W at a heatsink temperature of 200 K. Based on preliminary experimental results of the MTAE prototype, the following accomplishments were achieved:

- Operability of the MTAE at a cryogenic temperature of 77 K was demonstrated with helium;
- The existence of the thermoacoustic mechanism in the micron-scale channels of the MTAE at 77K was examined and verified as able to transport heat flux over a 180 K temperature difference to a 280 K heatsink using the miniature resonant tube bundles;
- Cooling power and heat rejection capability of the MTAE prototype were demonstrated using helium supply gas and a 77 K cold-stage temperature;
- The cooling power was obtained at 77 K with helium supply gas, which is above the J-T inversion temperature where temperature increases after expansion through a J-T.

This experimental study on MTAE heat rejection successfully demonstrated the feasibility of this technology applied in miniature cryocoolers at 77 K in both cooling power production and heat flux transportation that is driven by acoustic wave systems using the MTAE mechanism. Further work on the development of this technology aims to scale down the prototype channel and resonant tube into micro-scale and test its feasibility in a lower temperature range (below 40 K).

ACKNOWLEDGMENT

This project was funded by a DoD SBIR Phase II program under contract with the MDA DoD. The authors would like to thank Mr. Jeff Raab and Mr. Michael Petach from NGST, and Dr. Chris Paine of JPL for their valuable suggestions and support of the MTAE cryogenic testing setup.

REFERENCES

1. P.E. Bradley, R. Radebaugh, M. Huber, and M.-H. Lin, ""Development of a Mixed-Refrigerant Joule-Thomson Microcryocooler," *Cryocoolers 15*, ICC Press, Boulder, CO (2009), pp. 425-432.
2. W. Chen and M. Zagarola,"Vibration-Free Joule-Thomson Cryocoolers for Distributed Microcooling," *Cryocoolers 15*, ICC Press, Boulder, CO (2009), pp. 433-440.
3. M.J. Simon, C. Deluca, V.M. Bright, Y.C.Lee, P.E. Bradley and R. Radebaugh, "Development of a Piezoelectric Microcompressor for a Joule-Thomson Microcryocooler," *Cryocoolers 15*, ICC Press, Boulder, CO (2009), pp. 441-450.
4. F. Roush and T. Roberts, "AFRL Space Cryogenic Technology Research Initiatives," *Cryocoolers 14*, ICC Press, Boulder, CO (2007), pp. 11-20.
5. R. Ross and R. Boyle, "An Overview of NASA Space Cryocooler Program-2006," *Cryocoolers 14*, ICC Press, Boulder, CO (2007), pp. 1-10.
6. D. Durand, R. Colbert, C. Jao and M. Michaelian, "NGST Advanced Cryocooler Technology Development Program (ACTDP) Cooler System," *Cryocoolers 14*, ICC Press, Boulder, CO (2007), pp. 21-31.
7. T. Nast, J. Olson, E.Roth, and B. Evtimov, "Development of Remote Cooling System for Low-Temperature Space-Borne Systems," *Cryocoolers 14*, ICC Press, Boulder, CO (2007), pp. 33-40.
8. M.V. Zagarola, W.L. Swift, H. Sixsmith, J.A. McCormick and M.G. Izenson, "Development of a turbo-Brayton cooler for 6K space applications," *Cryocoolers 12*, Kluwer Academic/Plenum Publishers, New York (2003), pp. 571-578.
9. G. Nellis, F. Dolan, J. McCormick, W. Swift, H. Sixsmith, J. Gibbon, and Castles, "Reveres Brayton cryocooler for NICMOS," *Cryocoolers 10*, Plenum Publishing Corp., New York (1999), pp. 431-438.
10. C. Knokel and W. Bradley, "Design and qualification of flight electronics for the HST NICMOS reverse Brayton cryocooler," *Cryocoolers 10*, Plenum Publishing Corp., New York (1999), pp. 439-448.
11. Zhimin Hu, "Thermoacoustic Expansion Valve: A New Type of Expander to Enhance Performance of Recuperative Cryocooler Systems," *Cryocoolers 14*, ICC Press, Boulder, CO (2007), pp. 429-436.
12. Zhimin Hu, "Cooling Performance of Miniaturized Thermoacoustic Expanders Operated at 133 K," *Cryocoolers 15*, ICC Press, Boulder, CO (2009), pp. 451-460.
13. J.A. McCormick, G. F. Nellis, W.L. Swift and H. Sixsmith, "Design and test of low capacity reverse Brayton Cryocooler for refrigeration at 35K and 60K," *Cryocoolers 10*, Plenum Publishing Corp., New York (1999), pp. 421-429.
14. G.F. Nellis, J.R. Maddocks, A. Kashani, J.H. Baik, and J.M. Pfotenhauer, "A first order model of a hybrid pulse tube/reverse-Brayton cryocooler," *Cryocoolers 12*, Kluwer Academic/Plenum Publishers, New York (2003), pp. 349-359.
15. J.A. McCormick, W.L. Swift and H. Sixsmith, "Progress on the development of miniature turbomachines for low-capacity reverse-Brayton cryocoolers," *Cryocoolers 9*, Plenum Press, New York (1997), pp. 475-483.
16. C.L. Hannnon and J. Gerstmann, M. Traum, J.G. Brisson, and J.L. Smith, Jr., "Development of a medium-scale Collins-type 10K cryocooler," *Cryocoolers 12*, Kluwer Academic/Plenum Publishers, New York (2003), pp. 587-594.